Cement and Concrete Research 39 (2009) 340–344

Contents lists available at ScienceDirect

Cement and Concrete Research

journal homepage: http://ees.elsevier.com/CEMCON/default.asp

Electrokinetic potential of hydrated cement in relation to adsorption of chlorides

Y. Elakneswaran *, T. Nawa, K. Kurumisawa

Division of Solid Waste, Resources and Geoenviromental Engineering, Graduate School of Engineering, Hokkaido University, Kita-Ku, Kita 13, Nishi 8, Sapporo, Hokkaido, 060-8628, Japan

ARTICLE INFO

Article history:
Received 18 August 2008
Accepted 18 January 2009

Keywords:
Chloride adsorption
Surface charge
Zeta potential
Cement
C–S–H
Surface complexation

ABSTRACT

In this study, surface charge mechanism of cement hydrates and its relations to adsorption of chloride ions are investigated. Hydrated cement paste (HCP) shows net positive surface charge by dissociation and adsorption. In HCP, chlorides bind as Friedel's salt (chemical binding) as well as adsorb on the surface of hydrates (physical binding). A surface complexation model is used to predict the adsorption of chlorides on calcium silicate hydrates (C–S–H). A good agreement between experimental and predicted chloride adsorption isotherm clearly demonstrate that the chlorides adsorb on the surface of C–S–H and bringing additional negative surface charge ($SiOHCl^-$). However, chloride ions neutralize the positively charged surfaces of portlandite and Friedel's salt by physical adsorption. From the results, it can be concluded that C–S–H is the dominant phase in terms of chloride adsorption in HCP.

1. Introduction

Chloride transport through cover concrete to embedded steel is responsible for corrosion problems in reinforced concrete structures exposed to marine environments or to the use of de-icing salt [1,2]. Chloride binding in cement hydrates influences the chloride ingress and chloride threshold level which determines the time to initiate the chloride induced corrosion [3,4]. Cement-based materials, like most other materials, acquire an electric charge when they left in contact with a polar medium. The electrical charges in hydrated phases are a consequence of both dissociation and the presence of charges at the surface due to ionic binding properties of surface groups [5–8]. Ingress of ions through pores of charged materials is influenced by nature of surface charge [9,10]. Authors identified the nature of surface charge of hydrated cement paste and its influence on diffusion of chloride ions [11]. A great number of studies are published on chloride ingress in cement-based materials [12–14]. In addition, studies about some influencing parameters on chloride binding capacity have also been well articulated [15,16]. However, there is a lack of knowledge on surface charge influences on chloride binding. Thus, this study focuses on mechanisms of chlorides interaction with cement hydrates. In particular, zeta potential measurements, chloride binding capacity, and pore structure analysis are presented in order to elucidate the link between electrokinetic potential and chloride adsorption.

2. Materials and methods

The compositions and physical properties of OPC (Ordinary Portland Cement) are given in Table 1. HCP (Hydrated Cement Paste) was prepared with water to cement ratio of 0.5 and cured in saturated calcium hydroxide solution until 91 days to avoid calcium leaching. De-ionized water was used as mixing water throughout the whole experiment. The cured sample was grounded by ball mill and fraction of particles having a diameter less than 45 μm was used for zeta potential (ζ) measurements. The X-ray diffraction (XRD) Rietveld analysis results of major phases in HCP are tabulated in Table 2. Aluminate (C_3A) phase was synthesized by mixing stoichiometric portions of calcium carbonate and aluminum oxide, and the mixture was burnt in a furnace at 1400 °C for 3 h. After cooling, the mixture was again mixed and burnt at the same condition [17]. Ettringite, monosulfate, Friedel's salt, and hydrogarnet were made by mixing of the synthesized C_3A with other materials according to Table 3 [17].

Pore solution in HCP was extracted using steel die method by applying pressures up to 250 MPa. Shortly after the extraction, chemical analyses were carried out on filtered solutions using ion chromatography and Inductively Coupled plasma (ICP) mass spectrometry. Mercury Intrusion Porosimetry (MIP) was used to determine the pore structure of HCP. Prior to the porosity measurement, the sample was immersed into acetone to stop its hydration and then vacuumed at 0.1 MPa for one day. The MIP equipment can generate the maximum pressure of 250 MPa and evaluate the pore diameter in the range of 6 nm to 0.1 mm. Specific surface area (BET method) and pore size distribution for smaller pores (BJH method) of HCP were determined by measuring isothermal nitrogen adsorption using Quantachrome Autosorb Automated Gas Sorption. The hydration was stopped as described in MIP test. Before the adsorption experiment, the sample was dried and outgassed.

* Corresponding author. Tel.: +81 11 706 6326; fax: +81 11 706 7274.
E-mail address: laknesh@eng.hokudai.ac.jp (Y. Elakneswaran).

0008-8846/$ – see front matter.
doi:10.1016/j.cemconres.2009.01.006

Table 1
Physical properties and compositions of OPC.

	OPC
Density (kg m^{-3})	3160
Blain surface area (m^2 kg^{-1})	325
LOI (%)	0.072
Chemical composition (wt.%)	
SiO_2	21.5
Al_2O_3	5.5
Fe_2O_3	2.9
CaO	64.3
MgO	1.9
SO_3	1.8
Na_2O	0.26
K_2O	0.38
Phase composition (wt.%)[a]	
C_3S	52.06
C_2S	22.45
C_3A	9.67
C_4AF	8.82
Gypsum	3.87

Nomenclature in cement chemistry: C = CaO, S = SiO_2, A = Al_2O_3, F = Fe_2O_3.
[a] Bogue calculations.

Suspensions of 0.1 g/l solid to liquid ratio were used for ζ measurements. The suspensions were kept for 2 h and then dispersed by ultrasonic waves for 1 min before the measurements. The ζ measurements were performed with Zetasizer Nano series. This apparatus calculates ζ by determining electrophoretic mobility and then applying Henry equation. Smoluchowski approximation was made during the measurements. Therefore, calculation of ζ from the mobility is straightforward for the system that fit the Smoluchowski model. For each suspension, the average ζ value was obtained from ten measurements.

Chloride binding capacity of HCP was conducted using equilibrium concentration technique [18]. After the curing period, HCP was crushed and sieved to provide samples of diameter between 0.5 mm and 2 mm. Around 25 g of the sample was immersed into known sodium chloride concentrations of 30 ml and those were tightly sealed to prevent carbonation and stored in room temperature for six months to reach adsorption equilibrium. The adopted sodium chloride concentrations were 1, 10, 100, 500, and 1000 mmol/l. Once the equilibrium reached, the inside solution was filtered, and chloride ion concentration was measured by use of ion chromatography. The chloride bound samples were grinded by ball mill, and those powders were used for XRD analysis to determine the amounts of Friedel's salt. The amounts of adsorbed chloride on the surface of HCP, Friedel's salt, and portlandite were determined from ionic concentration measurements. The sample was mixed with a known chloride solution at solid water ratio of 0.1 g/l and kept for 2 h. Then, the suspensions were centrifuged for 1 min and then those were filtered by using filter of 0.45 μm. The concentration of chloride ions in the filtered sample was measured by ion chromatography.

The surface potential and the amounts of adsorbed chlorides calculations were performed in PHREEQC using a surface complexation model including electrostatic term [19]. Assume that the HCP is considered as an assemblage of two main phases: C–S–H and portlandite, and mass percent of amorphous is equal to C–S–H mass percent (Table 2). Furthermore, the surface of C–S–H consists of only one type site (SiOH), and its density can be calculated according to the silicate structural model of C–S–H presented by Viallis-Terrisse H et al. [6]. In this model, three tetrahedral occupy a surface of 41 $Å^2$, and one among them carries two negative charges when completely dissociated. The specific surface area of C–S–H was assumed to 500 m^2/g.

Table 3
Synthetic condition of calcium aluminate hydrates [17].

Minerals	Chemical formula	Reagents			Curing condition	
		C_3A	$CaSO_4.2H_2O$	$CaCl_2$	Temp. (°C)	Time (days)
Ettringite	$3CaO.Al_2O_3.3CaSO_4.32\ H_2O$	√	√	—	50	30
Monosulfate	$3CaO.Al_2O_3.CaSO_4.12\ H_2O$	√	√	—	50	30
Friedel's salt	$3CaO.Al_2O_3.CaCl_2.10\ H_2O$	√	—	√	R.T	42
Hydrogarnet	$3CaO.Al_2O_3.\ 6\ H_2O$	√	—	—	R.T	30

*√: used; —: not used; R.T: Room temperature.

3. Results and discussion

Pore solution compositions of HCP are dominated by Na^+, K^+, and Ca^{2+} (Table 4). It is possible to calculate Debye length from the known concentration of pore solution and it is around 0.7 nm. However, electrical potential in the double layer vanishes at a distance five times of the Debye length [20]. This means that the pore diameter less than around 7 nm is fully covered with Electrical Double Layer (EDL). A chloride ion is always solvated by water molecules and its size higher than chloride ion. Several studies indicate that chloride ion is symmetrically solvated in clusters containing up to 255 water molecules, and the size of cluster might be around 2–3 nm [21,22]. Thus, EDL properties must give influence to transport of chloride through the pore diameter which is less than around 10 nm. Pore size distribution from MIP and nitrogen gas adsorption technique show more than 30% of the total pore volume of HCP has fallen in the pore diameter below 10 nm (Table 5). Thus, HCP has considerable amount of gel pores, and the interaction between electrokinetic properties and ingress of chloride ion cannot be negligible in the pores.

3.1. Mechanisms of surface charge creation in hydrated cement

Hydrated cement paste is considered as an assemblage of several phases. Each phase shows different surface characteristics when it contacts with water. The ζ values of HCP and its major phases in water are shown in Fig. 1. Friedel's salt and portlandite possess positive surface charge while others show negative surfaces in water. The principal hydration product of hydrated cement, C–S–H, consists of silicates and they have SiOH surface groups. Dissociation of silanol sites (SiOH) due to high pH in a solution gives a negative surface according to [5,6]

$$\equiv SiOH + OH^- \Leftrightarrow \equiv SiO^- + H_2O \quad (1)$$

Dissociation of both Friedel's salt and portlandite give positive surfaces according to [23,24]

$$Ca_2Al(OH)_6 \cdot Cl \cdot 2H_2O \Leftrightarrow [Ca_2Al(OH)_6]^+ + [Cl \cdot 2H_2O]^- \quad (2)$$

$$\equiv Ca(OH)_2 \Leftrightarrow \equiv [CaOH]^+ + OH^- \quad (3)$$

Ions in the pore solution are prone to interact strongly with silanol sites by an adsorption process. So, they can be considered afterward fixed

Table 2
XRD Rietveld analysis results of HCP.

	Weight (%)						
	Amorphous	Portlandite	AF_m	C_3S	C_2S	C_3A	C_4AF
HCP	73.76	11.54	0.30	9.61	3.19	0.45	0.04

Table 4
Pore solution concentrations of HCP.

Sample	Concentrations, mmol/l					Ionic strength, mmol/l	Debye Length, nm
	Na^+	K^+	Ca^{2+}	Cl^-	SO_4^{2-}		
HCP	88.9	74.8	4.8	1.4	0.2	178.3	0.72

Table 5
Pore size distribution.

		Pore volume, cm^3/g (%)					
		By Nitrogen adsorption	By MIP				
	Total	1.4–6 nm	6–10 nm	10–50 nm	50–100 nm	100–1000 nm	>1000 nm
HCP	0.1460	0.012 (8.2)	0.0324 (22.2)	0.0709 (48.6)	0.0198 (13.6)	0.0035 (2.4)	0.0074 (5.1)

on silanol sites. A physical adsorption of pore solution ions on C–S–H surface is represented as [6,25]:

$$\equiv SiOH + Ca^{2+} \Leftrightarrow \equiv SiOCa^{+} + H^{+} \quad (4)$$

$$\equiv SiOH + Ca^{2+} + SO_4^{2-} \Leftrightarrow \equiv SiOCaSO_4^{-} + H^{+} \quad (5)$$

$$\equiv SiOH + Ca^{2+} + Cl^{-} \Leftrightarrow \equiv SiOCaCl + H^{+} \quad (6)$$

The electrokinetic behavior of hydrated cement can be changed depending on the extension of ion adsorption, i.e. ionic concentration in the pore solution. Several studies indicate that the calcium ions constitute as potential determining ions on C–S–H surface and leading to charge reversal [6,7]. Surface potential (ψ) of C–S–H can be calculated from the surface potential of HCP and portlandite [5].

$$\psi_{HCP} = \frac{\psi_{C-S-H} * m_{C-S-H} * s_{C-S-H} + \varsigma_{CH} * m_{CH} * s_{CH}}{m_{C-S-H} * s_{C-S-H} + * m_{CH} * s_{CH}} \quad (7)$$

Where ψ_{HCP} and ψ_{C-S-H} are surface potential of HCP and C–S–H respectively, ζ_{CH} is zeta potential of portlandite, m_{C-S-H} and m_{CH} are mass percent of C–S–H and portlandite respectively, s_{C-S-H} and s_{CH} are specific surface area of C–S–H and portlandite respectively. Measured BET specific surface area of portlandite was 14.31 m^2/g. Fig. 2 shows the surface potential deduced from Eq. (7) for C–S–H in different calcium hydroxide concentrations compared with ψ_{C-S-H} obtained from surface complexation model. Both ζ and ψ do not represent the same potential: ζ is the electrical potential at the shear plane, whereas ψ is the theoretical potential of solid surface. In HCP, the difference between ζ and ψ is important for high ionic strength (higher than 0.1 M) and high ψ (higher than 25 mV in absolute value) [5]. In this study, the discrepancy between ζ and ψ is small and both potentials can be comparable. Experimental values are good

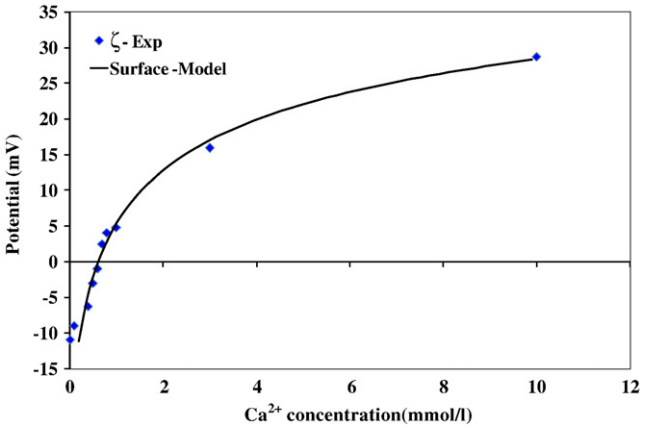

Fig. 2. Measured zeta potential and calculated surface potential of C–S–H as a function of calcium concentration.

agreement with model, and log*K* values for Eqs. (1) and (4) are −12.7 and −9.4 respectively. However, Viallis-Terrisse et al. [6] have calculated log*K* values for Eqs. (1) and (4) for synthetic C–S–H are −12.3 and −9.4 respectively, and Pointeau's et al. [5] calculated values are −12.0 and −9.2 respectively. These equilibrium constants values depend on the calcium-silicon ratio of C–S–H. The most likely candidate for adsorption of calcium is C–S–H. Having a high specific surface area and mass percent, the surface potential of HCP is controlled by C–S–H. As a high concentration of calcium and low concentration of sulfate in the pore solution (Table 4), the surface of hydrated cement is positive. This net positive surface charge concentration of hydrated cement paste can be determined by membrane potential measurements [11,26], and it is equal to 6.85 mmol/l. The interaction between chlorides and cement hydrates might influence the surface charge.

3.2. Chemical binding of chlorides in HCP

It is assumed that the chemical binding mechanism is due to conversion of hydroxyl AFm to chloride AFm (Friedel's salt) by ion exchange [27]. XRD Rietveld analysis was carried out to determine the amounts of Friedel's salt in the chloride bound HCP. The chloride binding isotherm (by equilibrium concentration technique) and chemical binding of chloride (by XRD Rietveld analysis) are shown in Fig. 3. The higher the total concentrations of chlorides the more chlorides are bound and the relationship between total and bound

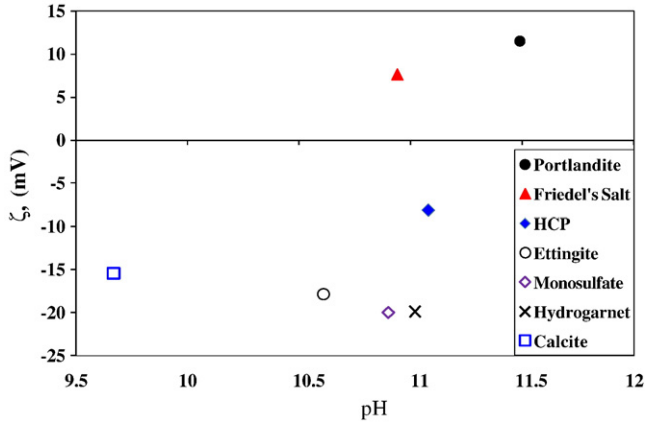

Fig. 1. Zeta potential of particles in water.

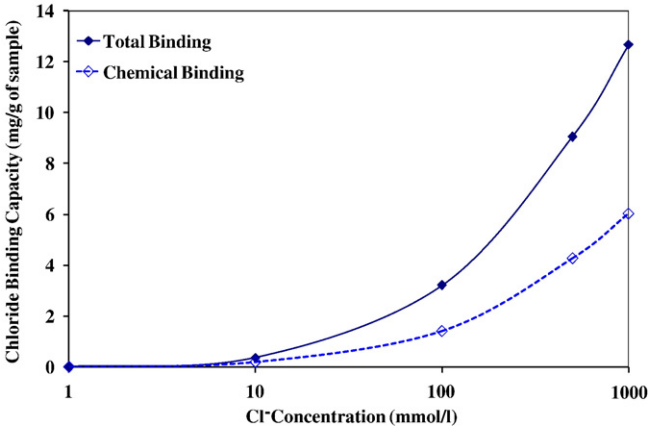

Fig. 3. Chloride binding isotherm and chemical binding of chloride for HCP.

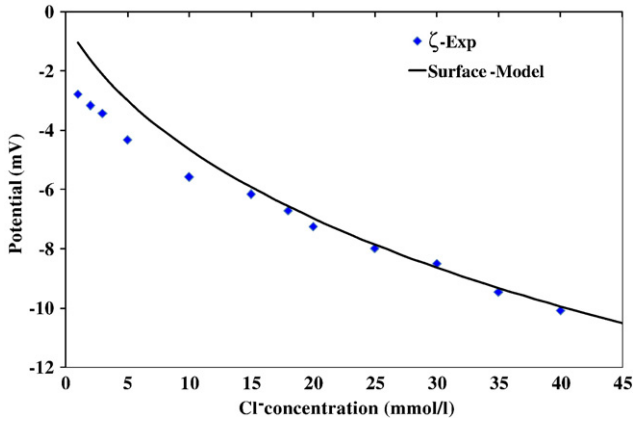

Fig. 4. Measured zeta potential and calculated surface potential of C–S–H in $Ca(OH)_2$ (Ca^{2+} concentration is equal to IEP of Ca^{2+}) with varying NaCl concentration.

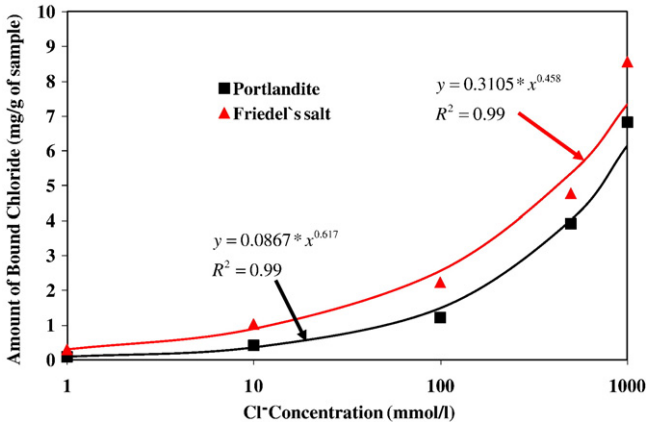

Fig. 6. Amount of adsorbed chloride vs. initial chloride concentration for portlandite and Friedel's salt.

chlorides is non-linear. Thus, both chemical and physical binding of chlorides are believed to occur in the HCP.

3.3. Physical adsorption of chlorides with cement hydrates

Physical adsorption is caused mainly by van der Waals attraction and electrostatic forces between chlorides and cement hydrates. The physical adsorption of ions onto the surface of cement hydrates depends on the surface properties, specifically the surface charge. Degrees of dissociation of SiOH surface groups vary from 10 to 90% when an increase of calcium hydroxide solution from 1 mmol/l (≈ pH 10) to 20 mmol/l (≈ pH 12.5) [28]. In sodium chloride solution (≈ pH 11.1), sodium behaves as indifferent ion (i.e. it does not adsorb on the surface of cement hydrates) towards the surface C–S–H [6,7]. Part of SiOH surface groups can be dissociated according to Eq. (1), and chloride can make an ionic bond with unionized SiOH through the reaction:

$$\equiv SiOH + Cl^- \Leftrightarrow \equiv SiOHCl^- \quad (8)$$

Fig. 4 shows calculated surface potential of C–S–H with zeta potential of HCP in sodium chloride solutions, where the surface of HCP was neutralized by calcium before it contacted with sodium chloride. The evolution of surface potential due to chloride adsorption on C–S–H surface is very similar to the measured ζ value, and predicted log*K* for Eq. (8) is equal to −0.35. The ζ variation of Friedel's salt and portlandite in sodium chloride solution clearly indicates that the physical adsorption of chloride on their surfaces (Fig. 5). From the Eq. (2), Friedel's salt dissociate into water and the surface of $[Ca_2Al(OH)_6]^+$ is compensated by chloride ions in the solution.

$$[Ca_2Al(OH)_6]^+ + Cl^- + 2H_2O \Leftrightarrow [Ca_2Al(OH)_6]Cl \cdot 2H_2O \quad (9)$$

Chloride can be adsorbed on the positive surface of dissociated portlandite and forms CaOHCl. It is a crystal structure and can be detected by XRD [29].

$$\equiv [CaOH]^+ + Cl^- \Leftrightarrow \equiv CaOHCl \quad (10)$$

Thus, chloride behaves as specially adsorbed ion towards the positive surfaces of both Friedel's salt and portlandite, leading to reversal of ζ at high concentration of chlorides. Adsorption experiment verifies the results obtained by ζ measurements (Fig. 6), and both Portlandite and Friedel's salt follow Freundlich isotherm. Higher the specific surface area of Friedel's salt (measured BET surface area is 48.43 m^2/g) gives higher ability of chloride adsorption than portlandite. This is an agreement with molecular dynamics modeling; the chloride binding capacity decrease in the sequence Friedel's salt > portlandite > ettringite > tobermorite [30]. The chloride adsorption on the surface of HCP is contributed by the adsorption on each cement hydrate phase. Physical adsorption of chlorides on the surface of HCP gives additional negative charge, leads to more negative value of ζ with increase of chloride concentration (Fig. 5). The increase of chlorides at first causes an increase of absolute value of ζ by adsorption, but at higher concentrations of chloride the chloride itself begins to contribute to the ionic strength and ζ is diminished in magnitude. Fig. 7 shows predicted

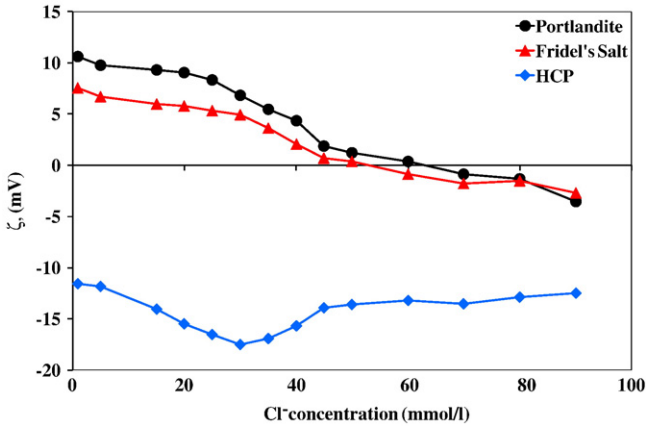

Fig. 5. Zeta potential of portlandite, Friedel's salt, and HCP in NaCl solution.

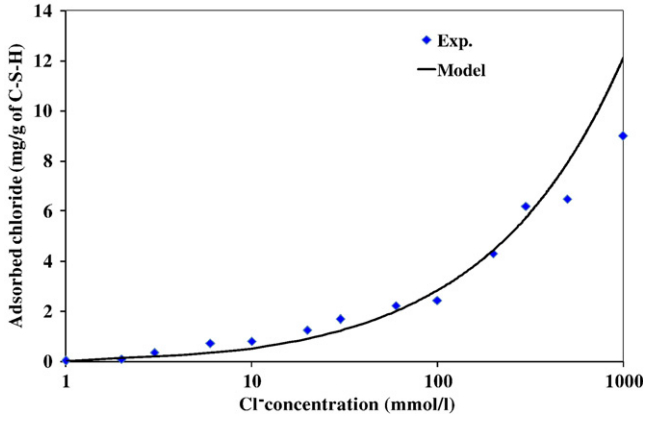

Fig. 7. Comparison between experimental and simulated Cl^- adsorption on C–S–H surface.

and experimental physical adsorption of chloride on C–S–H surface. The experimental physical adsorption of chloride on C–S–H was deduced from the chloride binding isotherm of HCP (Fig. 3) and portlandite (Fig. 6). In addition, physical adsorptions of chlorides are from adsorption experiments. C–S–H, having a high specific surface area and major constituent in HCP, dominates the physical binding of chloride in HCP. The amounts of adsorbed chloride at equilibrium per unit mass of C–S–H increases with increasing equilibrium chloride concentration. This result demonstrates that the surface of C–S–H becomes negatively charged by adsorption of chlorides. Alkaline cations are able to bind on C–S–H surface with chloride. The adsorbability of cations on the surface of HCP decrease in order: $Ca^{2+} > Cs^{+} > K^{+} > Na^{+}$, and adsorption of anions on HCP is: $SO_4^{2-} > Cl^{-}$ [31]. The concentration of suspensions will influence the ion-solid interaction. More accurate model and experiments are needed to understand the behavior of ionic species on the surface of cement hydrates.

4. Conclusions

Hydrated cement paste consists of high amount of gel pores, and its electrokinetic properties are increasingly recognized in chloride ingress. The surface charge of HCP is controlled by dissociation of cementitious phases and adsorption of ions. HCP possesses positive surface charge due to high concentration of calcium in the pore solution. Regarding the mechanisms of chloride binding in HCP, chemical binding is occurred by the reaction of chloride with hydrated cement phase (i.e. Friedel's salt formation); while physical binding is due to ionic adsorption on the surface. Portlandite and Friedel's salt possess positively charged surfaces by dissociation and have ability to adsorb chlorides physically. However, physical adsorption of chlorides in HCP is dominated by C–S–H. A surface complexation model was successfully used to predict the chloride adsorption on C–S–H surface. Physical adsorption of chlorides on the surface of C–S–H gives additional negative surface charge.

Acknowledgements

We would like to thank OPEN FACILITY (Hokkaido University Sousei Hall) for allowing us to use nitrogen adsorption experiment. Mr. H. Kawakami is gratefully acknowledged for his assistance in XRD Rietveld analysis.

References

[1] C.L. Page, Mechanisms of corrosion protection in reinforced concrete marine structure, Nature 256 (1975) 514–515.
[2] C.L. Page, K.W. J Treadaway, K.W.J. Treadaway, Aspects of the electrochemistry of steel in concrete, Nature 297 (1982) 109–115.
[3] G.K. Glass, N.R. Buenfeld, The influence of chloride binding on the chloride induced corrosion risk in reinforced concrete, Corrosion Science 42 (2000) 329–344.
[4] K.Y. Ann, H.W. Song, Chloride threshold level for corrosion of steel in concrete, Corrosion Science 49 (2007) 4113–4133.
[5] I. Pointeau, P. Reiller, N. Mace, et al., Measurement and modeling of the surface potential evaluation of hydrated cement pastes as a function of degradation, Journal of Colloid and Interface Science 300 (2006) 33–44.
[6] H. Viallis-Terrisse, A. Nonat, J.C. Petit, Zeta-Potential study of calcium silicate hydrates interacting with alkaline cations, Journal of Colloid and Interface Science 244 (2001) 58–65.
[7] L. Nachbaur, P.C. Nkinamubanzi, A. Nonat, et al., Electrokinetic properties which control the coagulation of silicate cement suspensions during early age hydration, Journal of Colloid and Interface Science 202 (1998) 261–268.
[8] H. Viallis, P. Faucon, J.C. Petit, et al., Interaction between Salts (NaCl, CsCl) and calcium silicate hydrates (C–S–H), Journal of Physical Chemistry B 103 (1999) 5212–5219.
[9] Andre Revil, Ionic diffusivity, electrical conductivity, membrane and thermo-electric potentials in colloids and granular porous media; a unified model, Journal of Colloid and Interface Science 212 (1999) 503–522.
[10] S. Chatterji, Aspects of ionic diffusion through thick matrices of charged particles, Journal of Colloid and Interface Science 300 (2006) 820–825.
[11] Y. Elakneswaran, T. Nawa, K. Kurumisawa, Influence of surface charge on ingress of chloride ion in hardened paste, Materials and Structures 42 (2009) 83–93.
[12] C.L. Page, N.R. Short, A. El. Tarras, Diffusion of chloride ions in hardened cement pastes, Cement and Concrete Research 11 (1981) 395–406.
[13] O.M. Jensen, P. F Hansen, A.M. Coats, F.P. Glasser, Chloride ingress in cement paste and mortar, Cement and Concrete Research 29 (1999) 1497–1504.
[14] C. Andrade, J. Kropp (Eds.), Testing and Modelling Chloride Ingress into Concrete, Proceedings of the 3rd International RILEM Workshop, Madrid, 2002.
[15] H. Zibara, R.D. Hooton, M.D.A. Thomas, K. Stanish, Influence of the C/S and C/A ratios of hydration products on the chloride ion binding capacity of lime-SF and lime-MK mixtures, Cement and Concrete Research 38 (2008) 422–426.
[16] C. Arya, Y. Xu, Effect of cement type on chloride binding and corrosion of steel in concrete, Cement and Concrete Research 25 (1995) 893–902.
[17] Y. Maeda, A. Ikeda, K. Haga, N. Sasaki, T. Ohma, The examination of dissolution of the cement hydrates and condition of an equilibrium calculation, TAIHEYO CEMENT KENKYU HOKOKU 149 (2005) 10–21 (in Japanese).
[18] R.K. Dhir, M.A.K. El-Mohr, T.D. Dyer, Chloride binding in GGBS concrete, Cement and Concrete Research 26 (1996) 1767–1773.
[19] D.L. Parkhurst, C.A.J. Appelo, User's guide to PHREEQC (Version 2) — a computer program for speciation, batch-reaction, one-dimensional transport and inverse geochemical calculations, Water-Resources Investigations Report 99-4259, U.S. Geological Survey, 1999.
[20] S. Chatterji, M. Kawamura, Electrical double layer, ion transport and reactions in hardened cement paste, Cement and Concrete Research 22 (1992) 774–782.
[21] S.J. Stuart, B.J. Berne, Surface curvature effects in the aqueous ionic salvation of the chloride ion, Journal of Physical Chemistry A 103 (1999) 10300–10307.
[22] S.J. Stuart, B.J. Berne, Effects of polarizability on the hydration of the chloride ion, Journal of Physical Chemistry 100 (1996) 11934–11943.
[23] M.R. Jones, et al., Studies using ^{27} Al MAS NMR of AF_m and Af_t phases and the formation of Friedel's salt, Cement and Concrete Research 33 (2003) 177–182.
[24] K. Popov, I. Glazkova, S. Myagkov, A. Petrov, E. Sedykh, L. Bannykh, V. Yachmenev, Zeta potential of concrete in presence of chelating agents, Colloids and Surfaces. A, Physicochemical and Engineering Aspects 299 (2007) 198–202.
[25] Y. Hosokawa, K. Yamada, B.F. Johannesson, L.O. Nilsson, Reproduction of chloride ion bindings in hardened cement paste using thermodynamic equilibrium models, in: RILEM Proceedings. 2nd International Symposium on Advances in Concrete Through Science and Engineering, 2006.
[26] Y. Elakneswaran, T. Nawa, K. Kurumisawa, Surface charge of hardened cement paste determined by membrane potential, Cement Science and Concrete Technology, Japan Cement Association 60 (2006) 111–117.
[27] F.P. Glasser, Role of chemical binding in diffusion and mass transport, in: R. Doug Hooton, et al., (Eds.), Proceeding Material Science of Concrete. International conference on ion and mass transport in cement-based materials, Toronto, 1999, pp. 129–154.
[28] C. Plassard, et al., Nanoscale experimental investigation of particle interactions at the origin of the cohesion of cement, Langmuir 21 (2005) 7263–7270.
[29] S. Saeki, et al., Effect of additives on dechlorination of PVC by mechanochemical treatment, J Mater Cycles Waste Manag, vol. 3, 2001, pp. 20–23.
[30] A.G. Kalinichev, R.J. Kirkpatrick, Molecular dynamics modelling of chloride binding to the surfaces of calcium hydroxide, hydrated calcium aluminates, and calcium silicate phases, Chemistry of Materials 14 (2002) 3539–3549.
[31] Y. Elakneswaran, T. Nawa, K. Kurumisawa, Influence of electrolytes on surface charge density of pastes, Cement Science and Concrete Technology, vol. 61, Japan Cement Association, 2007, pp. 108–114.